CONF-9505264--28

UCRL-JC-121614
PREPRINT

Diode-pumped Solid-State Laser Driver Experiments for Inertial Fusion Energy Applications

C. D. Marshall
S. A. Payne
M. E. Emanuel
L. K. Smith
H. T. Powell
W. F. Krupke

This paper was prepared for submittal to the
1st Annual International Conference on Solid-State Lasers
for Application to Inertial Confinement Fusion
Monterey, CA
May 30-June 2, 1995

July 11, 1995

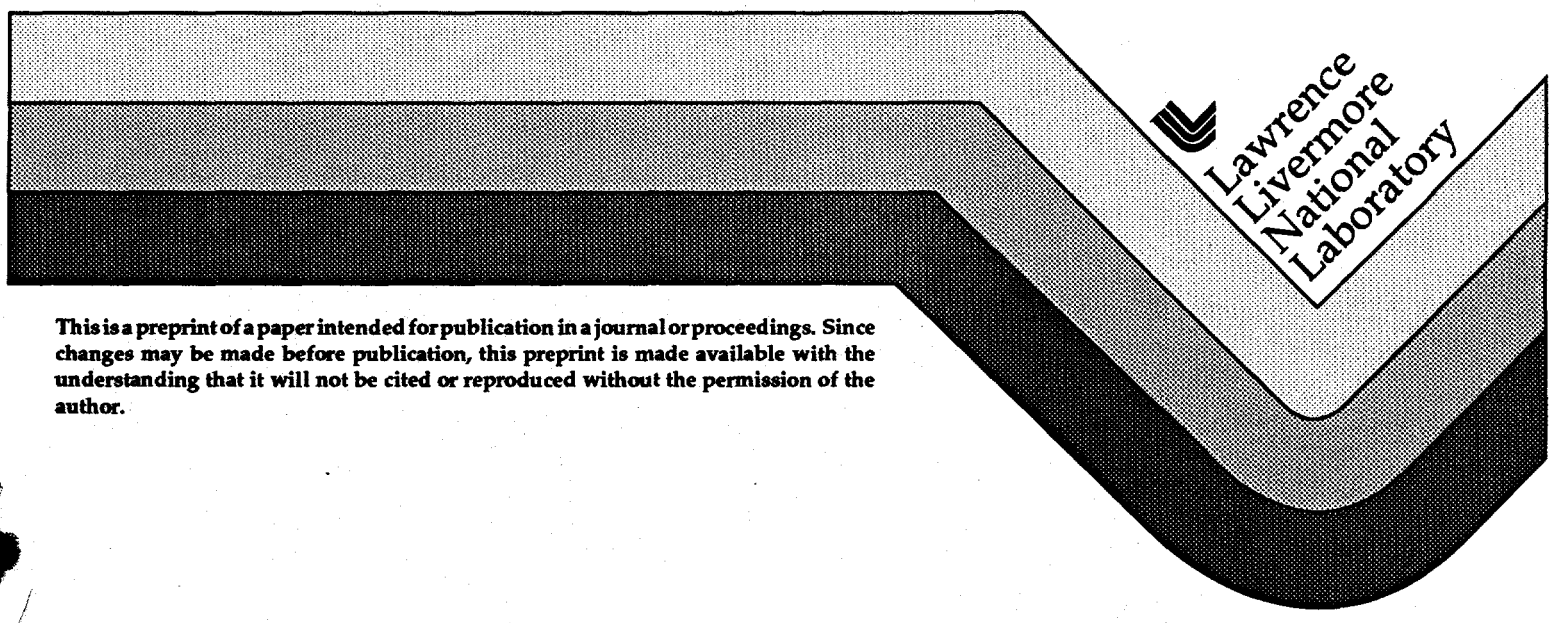

DISCLAIMER

Portions of this document may be illegible in electronic image products. Images are produced from the best available original document.

Diode-pumped solid-state laser driver experiments for inertial fusion energy applications

C. D. Marshall, S. A. Payne, M. E. Emanuel, L. K. Smith,
H. T. Powell, and W. F. Krupke
Lawrence Livermore National Laboratory, L-493, Livermore, CA 94551

Although solid-state lasers have been the primary means by which the physics of inertial confinement fusion (ICF) have been investigated, it was previously thought that solid-state laser technology could not offer adequate efficiencies for an inertial fusion energy (IFE) power plant. Orth and co-workers have recently designed a conceptual IFE power plant,[1] however, with a high efficiency diode-pumped solid-state laser (DPSSL) driver that utilized several recent innovations in laser technology. It was concluded that DPSSLs could offer adequate performance for IFE with reasonable assumptions. This system was based on a novel diode pumped Yb-doped $Sr_5(PO_4)_3F$ (Yb:S-FAP) amplifier. Because this is a relatively new gain medium,[2,3] a project was established to experimentally validate the diode-pumping and extraction dynamics of this system at the smallest reasonable scale. This paper reports on the initial experimental results of this study. We found the pumping dynamics and extraction cross-sections of Yb:S-FAP crystals to be similar to those previously inferred by purely spectroscopic techniques. The saturation fluence for pumping was measured to be 2.2 J/cm^2 using three different methods based on either the spatial, temporal, or energy transmission properties of a Yb:S-FAP rod. The small signal gain implies an emission cross section of 6.0×10^{-20} cm^2 that falls within error bars of the previously reported value of 7.3×10^{-20} cm^2, obtained from spectroscopic techniques. Up to 1.7 J/cm^3 of stored energy density was achieved in a 6x6x44 mm^3 Yb:S-FAP amplifier rod. In a free running configuration diode-pumped slope efficiencies up to 43% were observed with output energies up to ~0.5 J per 1 ms pulse from a 3x3x30 mm^3 rod. When the rod was mounted in a copper block for cooling, 13 W of average power was produced with power supply limited operation at 70 Hz with 500 μs pulses.

I. Introduction

Yb^{3+} based lasers have received substantial attention over the past several years. For example, Fan and coworkers[4] have demonstrated efficient laser action in Yb:YAG, while DeLoach et. al.[2] have developed lasers based on Yb-doped fluoroapatite, as well as several of its crystalline derivatives. In addition, Hanna and coworkers[5] have investigated Yb-doped fiber lasers. Yb-based materials, which typically lase around 1 μm, are aided by the simple electronic structure of Yb^{3+} in that it has only two accessible electronic states, eliminating the detrimental impact of upconversion or excited state absorption. In addition, the inherently small quantum defect of ~10-15% has led to relatively large intrinsic laser slope efficiencies.[4, 2,5] One detriment intrinsic to Yb^{3+} based lasers is that they operate as quasi-4-level systems since the terminal level can be thermally populated at room temperature. Although, if the pump source is sufficiently intense to effectively bleach the ground state, the laser will operate more like a true 4-level system. Laser diodes are the obvious choice as a high irradiance pump source since the ~900-1000 nm pump region for Yb-doped crystals and glasses overlaps with commonly available diode structures. The emission lifetimes of Yb-doped materials also tend to be significantly longer (> 1 ms) than Nd^{3+} doped into the same media, offering practical advantages in lowering the cost and increasing the effectiveness of diode laser pump sources. The above considerations suggest that diode-pumped solid-state Yb-lasers may provide significant advantages in efficiency and thermal performance over Nd-lasers for certain applications such as pulsed kJ class slab-laser systems that would be suitable as IFE drivers.

We believe that Yb:S-FAP is also particularly well adapted for certain laser applications that are sensitive to overall pumping and extraction efficiencies with ns pulses. Yb:S-FAP has a relatively low pump saturation intensity of 2.0 kW/cm^2 which is well suited to readily achievable diode array irradiances. In contrast, Yb:YAG has a pump saturation intensity of 28 kW/cm^2, which is more difficult to exceed, although Yb:YAG does offer significantly better thermal properties that are more desirable for high average power applications. Yb:S-FAP also offers a laser extraction fluence of 3 J/cm^2 that is compatible with typical ns laser damage thresholds of 10 to 20 J/cm^2.

II. Yb:S-FAP crystal growth

Methods for producing high quality S-FAP crystalline boules have been developed, up to 1" diameter by 7" long, with Yb^{3+} concentrations of 1.2×10^{19} cm^{-3} based on Czochralski growth techniques. This concentration required 1% Yb by weight in the starting melt. By post growth annealing the crystals for

This work was performed under the auspices of the U.S. Department of Energy by Lawrence Livermore National Laboratory under contract No. W-7405-Eng-48.

several days at ~300 K below the melting point, it was possible to routinely produce crystals with ~0.1%/cm scatter loss and ~1%/cm parasitic absorption at the emission wavelength.[3]

III. Pumping and extraction cross sections

In addition to the diode pumped Yb:S-FAP work described below, experiments were performed on Yb:S-FAP crystals using a tunable free running Cr:LiSAF laser as a diode surrogate with well defined spatial and spectral characteristics. The Cr:LiSAF oscillator was run as an unstable resonator and employed a 6 by 80 mm laser rod that was single flashlamp pumped. A dual-plate birefringent element was utilized for wavelength tuning. This laser, set to operate at 900 nm with a bandwidth of <0.5 nm, delivered up to 1.2 J of output energy for these experiments with a 1/e pulse width of 250 μs. A 50-cm lens was used to image relay the flat-top output of the oscillator into the Yb:S-FAP samples under test. The spatial profile at the sample location had 1/e beam diameter of 3.1 mm. In addition, a variable wave-plate and polarizer were utilized to attenuate the beam for fluence-dependent experiments.

A 6x6x44 mm^3 rectangular Yb:S-FAP crystal, with the c-axis (high-gain axis) set parallel to the 6x6 mm square faces which had a 3° wedge angle between the two square ends (to reduce parasitic oscillations), was utilized to investigate the pump dynamics, and the effect of the highly anisotropic gain and amplification. The two long sides with surface normal perpendicular to the c-axis were also ground to limit parasitic oscillation. A more detailed description of parasitic suppression, which is anisotropic due to the strongly polarized emission shown was discussed previously.[4]

The fractional transmission T of the π-polarized pump light observed by pumping the wedged Yb:S-FAP parallelepiped along the long axis, with the Cr:LiSAF laser described above, is shown in Fig. 1.

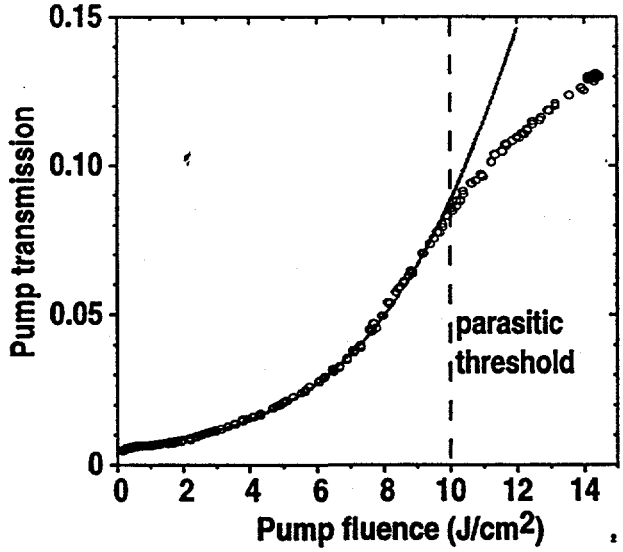

Figure 1. Fractional transmission of 6x6x44 mm Yb:S-FAP rod for a 900 nm 250 μs pump beam from a Cr:LiSAF laser. The solid lines are a best fit using Eq. 1 with a saturation fluence of 2.2J/cm^2 limit that the pump laser pulse length (~0.25 ms) is much shorter than the lifetime of the Yb:S-FAP (~1.26 ms)

A straightforward Frantz-Nodvik analysis can be utilized to model the saturated pumping. In this limit the transmission T is

$$T = \frac{F_{sat}}{F}\ln\left[1+\left\{\exp(F/F_{sat})-1\right\}\exp(-N_o h\nu L/F_{sat})\right] \qquad (1)$$

where F is the fluence of the 900-nm pump light (corrected for reflection losses), F_{sat} is the pump saturation fluence, N_o is the number density of Yb^{3+} ions, and L is the rod length. Using Eq. 1 it was possible to fit the transmission data in Fig. 1 up to ~10 J/cm^2, where the onset of soft parasitic modes produces a deviation from ideal behavior due to partial clamping of the excited-state population density (which reduces bleaching). The presence of soft parasitic modes above 10 J/cm^2 is not unexpected since such parasitic modes are frequently encountered in other gain materials in rod configurations that have significant gain (~10 single pass). The observed threshold for parasitics consistent with a pump fluence that can be used for efficient operation (I_{pump} = ~10 I_{sat} of Yb:S-FAP) of the rod amplifier geometry employed here.

The pump saturation fluence was determined to be 2.2 J/cm^2 from a numerical fit shown in Fig. 1, which used Eq. 1 and two adjustable parameters, N_o and F_{sat}. This experimental saturation fluence is in reasonable agreement with the predicted saturation fluence, defined as $h\nu/\sigma_{abs}$, of 2.5 J/cm^2 derived from previously reported values for the absorption cross section.[2] The Yb^{3+} concentration of N_o =1.3x10^{19} cm^{-3} determined from the least squares fit is also in reasonable agreement with the expected concentration of 1.1x10^{19} cm^{-3} determined from the absorption spectrum and the experimentally measured cross sections.

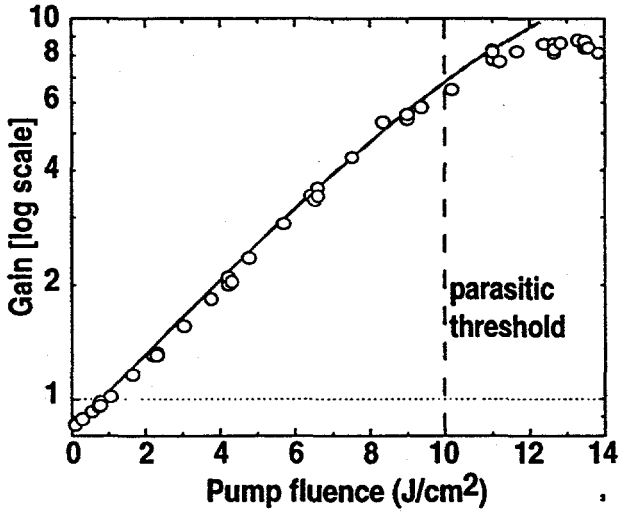

Figure 2. Single pass π-polarized small signal gain of Yb:S-FAP at 1047 nm versus pump fluence of a 250 μs pulse at 900 nm. A Cr:LiSAF pump laser was utilized due to its relatively narrow bandwidth and short pulse width so that accurate determinations of the saturation fluence could be made.

The Yb:S-FAP small signal gain was also measured under the same Cr:LiSAF excitation conditions by observing the single pass gain of a weak ~20 mW CW Nd:YLF probe laser that was either σ or π polarized in the S-FAP crystal. A Nd:YLF laser was chosen as the probe beam since the peak of the emission spectrum of Yb:S-FAP (1047.5 nm in air) overlaps with a common Nd:YLF laser line to within 0.1 nm. The cw probe beam was counter-propagated relative to the Cr:LiSAF pump beam with a 1/e diameter of 200 μm. A photodiode, 1047 nm bandpass filter, and transient digitizer were then used to measure the peak small signal gain as shown in Fig. 2. Using a straightforward numerical model which includes the temporal and spatial evolution of the ground and excited states in the presence of the Cr:LiSAF pump pulse, the polarized small signal gain was fit and is shown as solid lines in Fig. 2. The emission cross sections obtained from the fits were 6.0±1.0 and 1.45±0.2 x10^{-20} cm^2, for π and σ-polarizations, respectively. This is in reasonable agreement with the previously reported values of the emission cross section of 7.3 and 1.45 x10^{-20} cm^2 for π and σ-polarizations, respectively.[2]

IV. Laser diode pump array

An InGaAs laser diode array that has suitable characteristics for pumping a 3x3x30 mm Yb:S-FAP rod was also fabricated. The diode array emits 2.8 kW peak power from a package of 22 diode bars, each 1.5 cm in width and mounted on a microchannel cooled heatsink with a stacking pitch of 0.1 cm.

The laser diode wafers were grown by metalorganic chemical vapor deposition (MOCVD) [6] at 800°C and 20 mB chamber pressure. The active region of the device was a single 100 Å $In_{0.5}Ga_{0.95}As$ quantum well surrounded by 2000 Å $Al_xGa_{1-x}As$ graded regions (x = 0.6 to 0.3) and 1.4 μm $Al_{0.6}Ga_{0.4}As$ cladding layers and is similar to previously reported strained InGaAs quantum well lasers [7]. Notable is the absence of GaAs barrier layers surrounding the well which, at the operating wavelength of 900 nm, would be extremely lossy (~75 cm^{-1}) [8], making their inclusion near the active region of the device undesirable. Uncoated test devices (100 x 500 μm) exhibited ~258 A/cm^2 threshold current density and ~39% differential quantum efficiency per facet under 1 Hz, 100 μsec excitation.

Bars were fabricated using conventional techniques. Emitters were 100 μm wide on 140 μm centers, with an optical isolation trench etched between emitters to inhibit parasitic lasing and amplified spontaneous

emission effects. Wafers were cleaved into 15 mm bars with 1 mm cavity length and HR/LR coated. Bars were bonded to microchannel-cooled heatsinks and a cylindrical microlens was mounted on each assembly to collimate the beam in the direction normal to the plane of the junction. A diagram of the completed assembly is given in Fig. 3; details have been reported previously [9].

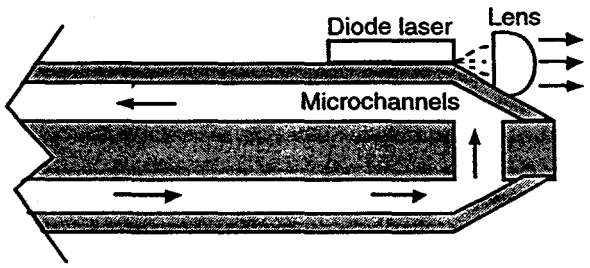

Figure 3. Cross-sectional view of a microchannel-cooled laser diode package with a conditioning microlens attached.

The diode output energy in a 1 ms pulse versus drive current is shown in Fig. 4. The output of the 1.5x2.2 cm^2 diode array was concentrated down to 0.3x0.3 cm^2 with a lensing duct[5] to 23 kW/cm^2.

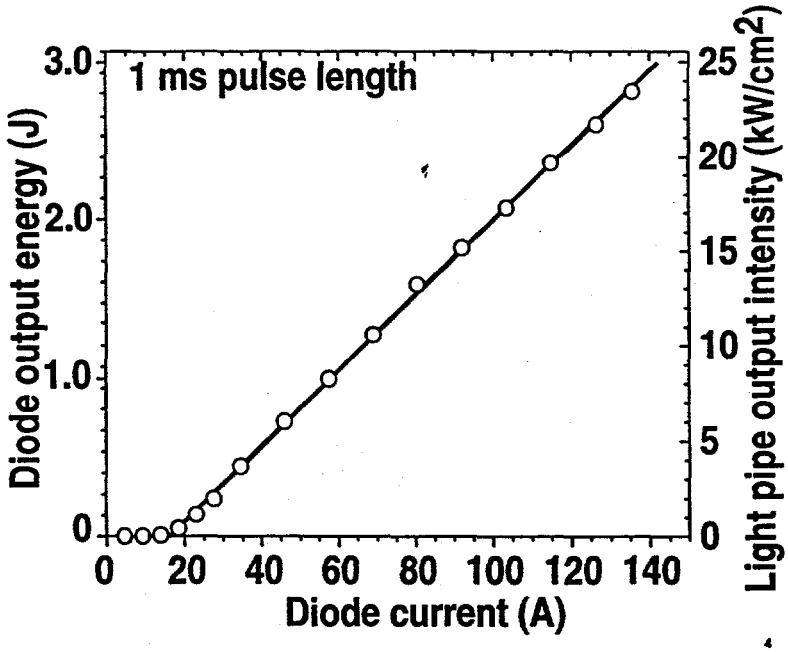

Figure 4. InGaAs laser diode array output energy versus diode drive current for a 22 bar stack of 1.5 cm linear diode bars. The output of the diode array emitting area was concentrated down by ~40X with a lensing duct with 75% efficiency up to a maximum of 23 kW/cm^2.

One particularly important requirement for the diodes is that the emission band width must be comparable with the relatively narrow 4 nm FWHM pumping band of Yb:S-FAP during a diode pulse that spans about one emission lifetime of Yb:S-FAP (1.10 ms). A suitable 6.5 nm FWHM diode emission bandwidth was accomplished simultaneously with other required specifications for Yb:S-FAP such as emission centered at 900.4 nm (at 12°C) when running with a 1 ms pulse length at 10 Hz and 2.8 kW peak emission power. Figure 5 presents the diode emission spectra described above overlaid with the transmission spectra of a 30 mm double passed Yb:S-FAP rod fabricated from the boule described above. Clearly most of the diode emission is absorbed into the gain medium in the absence of ground state bleaching and with the bleached pumping conditions utilized in the oscillator described below; ~75% absorption was achieved.

V. Diode pumped oscillator performance

A free-running Yb:S-FAP oscillator was constructed and diode-pumped through an external lensing duct[5] delivery system which concentrated the diode light intensity. The pumped end of the Yb:S-FAP rod had a short pass coating while the other end of the crystal was had a long-pass coating such that most of the pump light was retro-reflected down the rod for a second pass. Initial results were obtained with five different output coupler reflectivities ranging from 68% to 97%, all with a 75 cm concave radius of curvature. The 76% reflective output coupler was found to produce the highest output energies of 0.55 J with a 1 ms pump pulse length. Since only radiative air cooling was present in the above test, the laser was run at 1 Hz to prevent fracture, although work at higher repetition rate is discussed later in this article. Figure 6 presents the output energy from the oscillator constructed with the R=76% output coupler as a function of diode energy incident on the Yb:S-FAP rod. The diode input electrical energy is also plotted on the top axis. The slope of the oscillator output energy as a function of absorbed pump energy (laser slope efficiency) was measured to be 43% while the overall electrical slope efficiency was observed to be 9.1%.

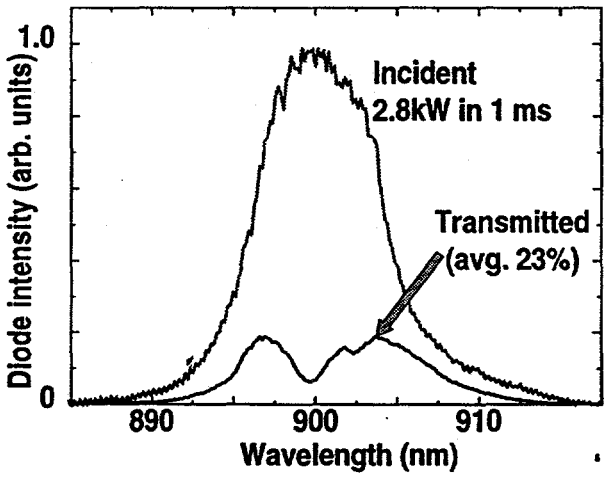

Figure 5. InGaAs laser diode array spectrum both incident on and transmitted through a 3x3x30 mm Yb:S-FAP rod with 1.2×10^{19} Yb/cm^3.

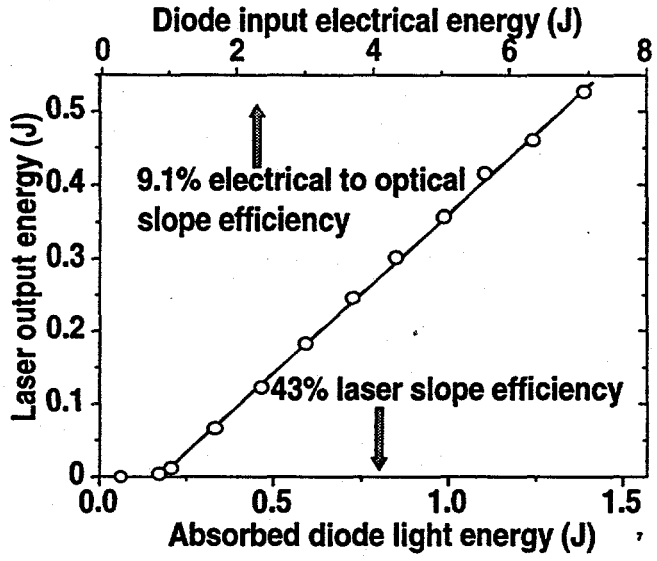

Figure 6. Diode-pumped Yb:S-FAP free-running lase output energy as a function of both absorbed diode light and input diode electrical energy. Laser slope efficiencies of 43% and overall electrical efficiencies of 9.1% were observed.

From the slope efficiency data obtained with a variety of output couplers, a Findley-Clay analysis was performed. Cavity losses can be estimated by plotting the logarithm of the output coupler reflectivity versus the lasing threshold as shown in Figure 7. The output coupler reflectivity R, laser threshold P_{th} are related via the expression

$$-\ln(R) = aP_{th} - (L_{ext} + L_{\text{int}}) \qquad (2)$$

where L_{ext} and L_{int} are the extrinsic (e.g. impurity absorption) and intrinsic (quasi-four-level) losses respectively. Using Eq. 2, the data in Fig. 6 imply a total round trip loss (RTL) of 37.7%. By subtracting the measured coating RTL of 6.1% and the quasi-4-level RTL of 3.2%/cm leads to L_{ext}=2.1%/cm extrinsic losses. This is comparable to the measured absorption and scatter loss of 1.1%/cm, although there appears to be ~1%/cm loss unaccounted for. Perhaps this is due to fill factor considerations in the cavity.

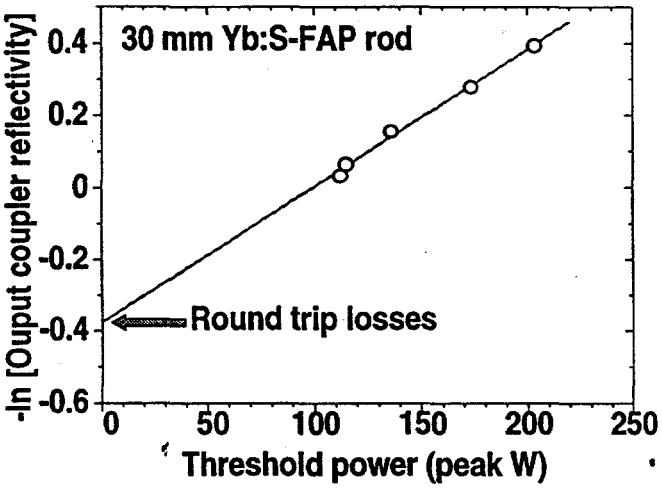

Figure 7. Logarithm of output coupler reflectivity versus threshold power of a diode-pumped free-running oscillator cavity. The intercept provides a measure of the total cavity losses.

An alternative method for obtaining similar cavity loss information is to plot the inverse slope efficiency η versus the inverse output coupling T as shown in Fig. 8. These parameters are related by

$$1/\eta = 1/\eta_o + L_{ext}/(T\,\eta_o) \qquad (3)$$

where η_o is the intrinsic laser slope efficiency (for zero cavity losses). The inverse intercept yields η_o=76% which is close to the ideal expected value of 86% (=900nm/1047nm) defined by the quantum defect. The slope times η_o leads to extrinsic cavity losses of 2.8%/cm after the known coating losses of 6.1% are subtracted. This extrinsic loss is similar to that obtained from the Findley-Clay analysis (2.1%/cm) described above. Consequently, we believe that future improvements in laser performance are possible with better rod coatings and less absorptive crystals at the laser emission wavelength.

A diode-pumped free-running oscillator was also constructed with the addition of active cooling. This was accomplished by encasing a rectangular 3x3x30 mm Yb:S-FAP rod that was thermally contacted to a copper block that was water cooled to 10 °C. By operating the diode array with a 120A 500 μs pulse at 70 Hz, up to 13 W of average power was produced as shown in Fig. 9. The maximum repetition rate was power supply limited and no rods were observed to fracture under these conditions even after prolonged operation. An oscillator running under similar conditions but at 10 Hz was observed to have 0.3% rms. pulse to pulse stability over one hour of operation and the long term amplitude drift was found to be less than 2% over a 14 hour period.

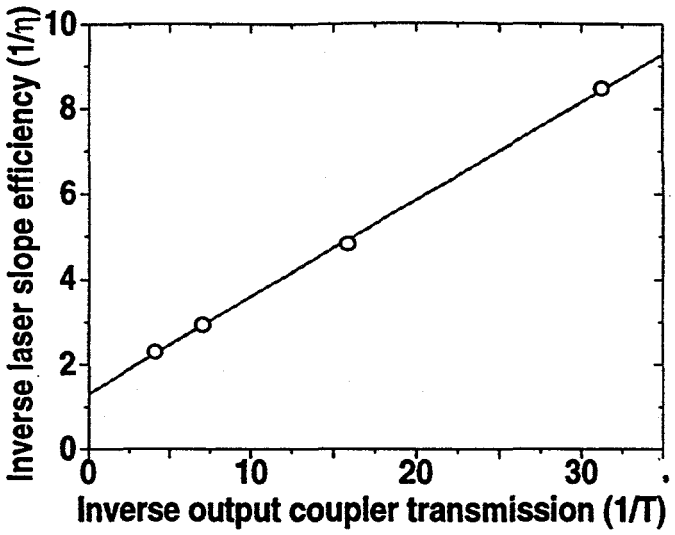

Figure 8. Diode-pumped Yb:S-FAP inverse laser slope efficiency versus inverse output coupler transmission for a diode-pumped free-running oscillator cavity. The Y-intercept and slope provide a measure of the intrinsic laser slope efficiency and the cavity losses, respectively

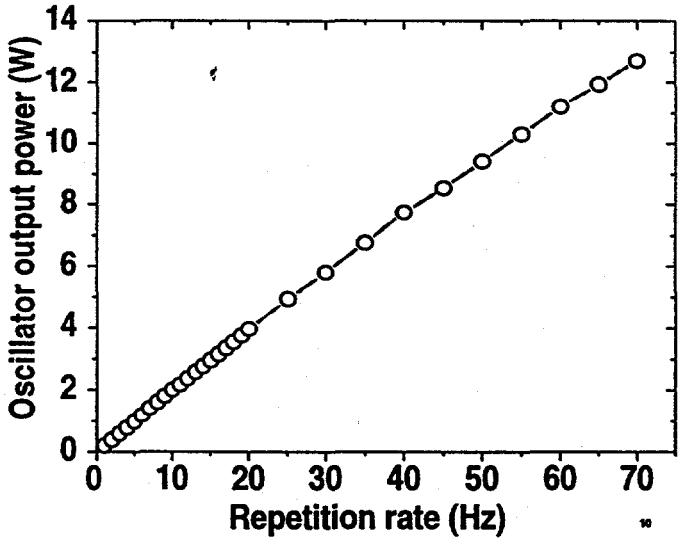

Figure 9. Diode-pumped copper block heat sinked Yb:S-FAP rod-oscillator operating at up to 70 Hz. A 500 μs pulse with 120A of drive current that corresponds to 63W of pump average power at 70 Hz were utilized.

VI. Summary

In summary, a diode-pumped Yb:S-FAP laser has been successfully demonstrated for the first time and favorable efficiencies were observed with up to 0.5 J of output in 1 ms from a 3x3x30 mm rod. This was obtained with a 2.8 kW InGaAs laser diode array operating at up to 4% duty cycle. Yb:S-FAP laser slope efficiencies up to 43% were observed and intrinsic laser efficiencies (no losses) were inferred to be 76%. The overall electrical to optical slope efficiencies were observed to be 9% for this first demonstration. Up to 13 W of average power were also obtained with the addition of active cooling to the rod. The basic spectroscopic properties previously reported were found to properly describe the physics of the laser media under operating laser conditions. The success of these experiments is very encouraging for the first demonstration of this DPSSL technology based on the novel Yb:S-FAP gain element. Further work promises to suitably improve this initial result and demonstrate that DPSSLs have a promising future as IFE drivers.

VII. Acknowledgments

We would like to thank B. Chai for providing the Yb:S-FAP crystals that were critical to this work. We would also like to thank L. DeLoach and K. Schaffers for sharing their technical expertise on the spectroscopic and crystal growth properties of Yb:S-FAP. We are also indebted to J. Tassano for constructing many of the laboratory facilities and to C. Orth for sharing his Yb:S-FAP amplifier system designs and calculations with us.

VIII. References

1. C. D. Orth, S. A. Payne and W. F. Krupke, Nuclear Fusion in press (1995).
2. L. D. DeLoach, S. A. Payne, L. K. Smith, W. L. Kway and W. F. Krupke, J. Opt. Soc. Am. B **11**, 269 (1994).
3. C. D. Marshall, S. A. Payne, L. K. Smith, H. T. Powell, W. F. Krupke and B. H. T. Chai, IEEE J. Selected Topics in Quantum Electronics **1**, 67 (1995).
4. T. Y. Fan, S. Klunk and G. Henein, Opt. Lett. **18**, 423 (1993).
5. C. J. Mackechnie, W. L. Barnes, D. C. Hanna and J. E. Townsend, Electron. Lett. **29**, 52 (1993).
6. H. M. Manasevit, Appl. Phys. Lett. **12**, 156 (1968).
7. C. A. Wang and H. K. Choi, IEEE J. Quantum Electronics **QE27**, 681 (1991).
8. D. Redfield and M. A. Afromowitz, Appl. Phys. Lett. **11**, 138 (1967).
9. R. J. Beach, M. A. Emanuel, W. J. Benett, B. L. Freitas, D. Ciarlo, N. W. Carlson, S. B. Sutton, J. A. Skidmore and R. W. Solarz, SPIE proceedings **2148**, 13 (1994).